LP_{01} to LP_{11} mode convertor based on side-polished small-core single-mode fiber*

LIU Yan (刘艳)[1,2]**, **LI Yang** (李阳)[1], **and LI Wei-dong** (李卫东)[1]

1. Key Lab of All Optical Network & Advanced Telecommunication Network, Ministry of Education, Beijing Jiaotong University, Beijing 100044, China

2. Institute of Lightwave Technology, Beijing Jiaotong University, Beijing 100044, China

(Received 26 October 2017; Revised 29 November 2017)

©Tianjin University of Technology and Springer-Verlag GmbH Germany, part of Springer Nature 2018

An all-fiber LP_{01}-LP_{11} mode convertor based on side-polished small-core single-mode fibers (SMFs) is numerically demonstrated. The linearly polarized incident beam in one arm experiences π shift through a fiber half waveplate, and the side-polished parts merge into an equivalent twin-core fiber (TCF) which spatially shapes the incident LP_{01} modes to the LP_{11} mode supported by the step-index few-mode fiber (FMF). Optimum conditions for the highest conversion efficiency are investigated using the beam propagation method (BPM) with an approximate efficiency as high as 96.7%. The proposed scheme can operate within a wide wavelength range from 1.3 μm to1.7 μm with overall conversion efficiency greater than 95%. The effective mode area and coupling loss are also characterized in detail by finite element method (FEM).

Document code: A **Article ID:** 1673-1905(2018)02-0088-4

DOI https://doi.org/10.1007/s11801-018-7234-7

The space-division multiplexing (SDM), represented by mode-division multiplexing (MDM), is considered as the breakthrough technique to overcome the future capacity-crunch of optical communication systems in recent years[1-6]. The guided modes in multimode fiber (MMF) or few-mode fiber (FMF) are orthogonal, which provides the opportunity of multiplexing different spatial modes as independent transmission channels to further increase the capacity. It is necessary to efficiently convert the source mode, typically LP_{01} mode in single-mode system, to target high-order modes supported by the transmission FMF. A straightforward way is using some free space components such as phase plate[1,2,7-10]. However, the free space bulk optical components not only are expensive and lossy, but also make it difficult to increase the number of spatial modes. Therefore, compact, low cost and integratable all-fiber mode convertors have attracted a great deal of attention. Several schemes, such as long-period gratings[11-13], micro-structure fiber devices[14-16], spot-based mode excitation[17] and multimode interference effect[18], have been demonstrated. The basic principle of the long-period grating schemes is to create a periodic perturbation which is capable of supporting resonant coupling between two transverse modes. The induced gratings could be achieved by various techniques, such as mechanical stress, acoustic waves, laser pulses or electro-optical effects. However, the long-period grating approach bears the drawback of limited bandwidth due to the wavelength-sensitive coupling. In the micro-structure fiber devices, the mode conversion relies on adiabatic propagation rather than resonant coupling enabling high extinction and wide wavelength range operation. But efficient coupling between the photonic crystal fiber (PCF) and the FMF that maintains modal purity is further required. The optical field distribution of an FMF can be described as a coherent superposition of all mode-fields supported by the fiber. Therefore, the spot-based mode coupler does not directly excite pure fiber modes, but excites a set of linear combinations of modes[17]. The all-fiber mode convertor based on multimode interference is essentially a mode excitation approach. For non-circularly symmetric modes, lateral offset in the fiber interfaces is further needed due to the circular symmetry of the fundamental LP_{01} mode in SMF. In this paper, an all-fiber LP_{01}-LP_{11} mode convertor based on side-polished small-core SMFs is proposed and numerically demonstrated. The side-polished parts merge into an equivalent TCF which spatially shapes the incident LP_{01} mode to the LP_{11} mode. Broadband operation, high conversion efficiency and low coupling loss are numerically demonstrated in C band.

The proposed all-fiber mode convertor is illustrated in Fig.1. The mode convertor consists of two identical small-core SMFs and a section of FMF, and the side-polished parts of small-core SMFs form the equivalent TCF. The small core fiber can be realized by

* This work has been supported by the Fundamental Research Funds for the Central Universities (No.2016JBM002).

** E-mail: bjtuly@163.com

pre-etching or pre-elongating of standard SMF. The source LP_{01} mode is split into two beams via a 3-dB coupler and propagates in each small-core SMF. The fundamental LP_{01} can actually be decomposed into two nondegenerate polarization modes. The birefringence induced by bending could become significant and produce a modification of the state of polarization after a long optical path. So, it's easier to coil a fiber with specific number of turns and radius to give a total delay between nondegenerate modes of π, which is analogous to fractional waveplates of classical optics. The linearly polarized beam in one arm experiences π shift through a fiber $\lambda/2$ waveplate[19]. And then, the combined beam in the TCF region has similar spatial profile to LP_{11} mode supported by the FMF. Due to the matched spatial profile, high conversion efficiency is obtained. It's worth mentioning that polarization-maintaining small-core SMFs are preferable, but fortunately, the polarization-maintaining property is still preserved in a compact design with normal fibers. Selective excitation of degenerate LP_{11} modes can be achieved by carefully adjusting the incident polarization to match the target mode. We use the power coupling coefficient to evaluate the conversion efficiency, which determines the amount of the input field power that couples to the LP_{11} mode in the FMF. In terms of an overlap integral in cylindrical coordinates, the power coupling coefficient can be determined using the following equation:

$$\eta = \frac{\left|\int_0^{\infty} E_s(r) E_{LP_{11}}(r)\, r\mathrm{d}r\right|^2}{\int_0^{\infty} \left|E_s(r)\right|^2 r\mathrm{d}r \int_0^{\infty} \left|E_{LP_{11}}(r)\right|^2 r\mathrm{d}r}, \quad (1)$$

where $E_s(r)$ and $E_{LP11}(r)$ represent the electric field of the optical beam launching from the TCF to the FMF, and the electric field of LP_{11} mode in FMF, respectively. From Eq.(1) we can see that if the source field has the same spatial profile as the target LP_{11} mode, η will be equal to 1, which means 100% conversion efficiency. Therefore, we attempt to optimize the three TCF parameters, including pitch D, diameter d and length L_{TCF}, to maximize the possible conversion efficiency. A beam propagation model is established according to Fig.1. And the related parameters are listed in Tab.1. The FMF used here has a step-index profile with normalized frequency of 3.61 μm at 1.55 μm, so the FMF only supports the LP_{01} and LP_{11} modes. Two linearly polarized beams with π shift are launched into the small-core SMFs, respectively. The length of the TCF is set as 100 μm and the operation wavelength is 1.55 μm. The pitch D and diameter d are scanned simultaneously and the power coupling coefficients as a function of these two parameters are shown in Fig.2(a). The maximum coupling coefficient locates at (0.32, 5.97) indicated by the black cross with the value of 0.96. And Fig.2(a) also denotes a loose requirement of the core distance and diameter to achieve a normalized power above 0.9. Then we choose the two optimized values and further scan the L_{TCF} as shown in Fig.2(b). As can be seen from Fig.2(b), with the L_{TCF} varying from 0 to 5 mm, the normalized power is always above 0.94. And some peaks are observed with the first two locating at 50.2 μm and 1 015.6 μm, and the corresponding power coupling coefficients are 0.97 and 0.95, respectively. Therefore, the conversion efficiency as high as ~96.7% can be achieved at 1.55 μm.

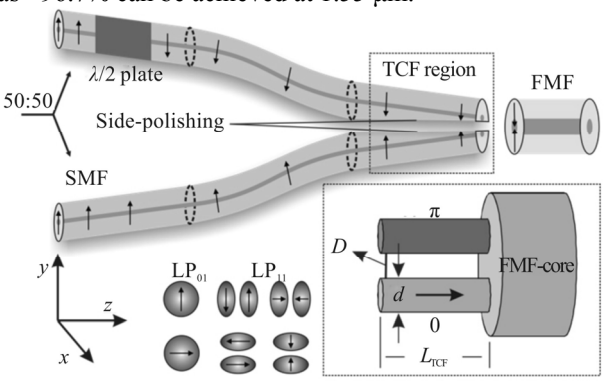

Fig.1 Schematic diagram of the proposed all-fiber LP11 mode convertor

Tab.1 Simulation parameters

	Core (μm)	Cladding (μm)	n_{core}	n_{clad}
SMF	d/2	62.5	1.450 5	1.444 0
FMF	6.5	62.5	1.450 5	1.444 0

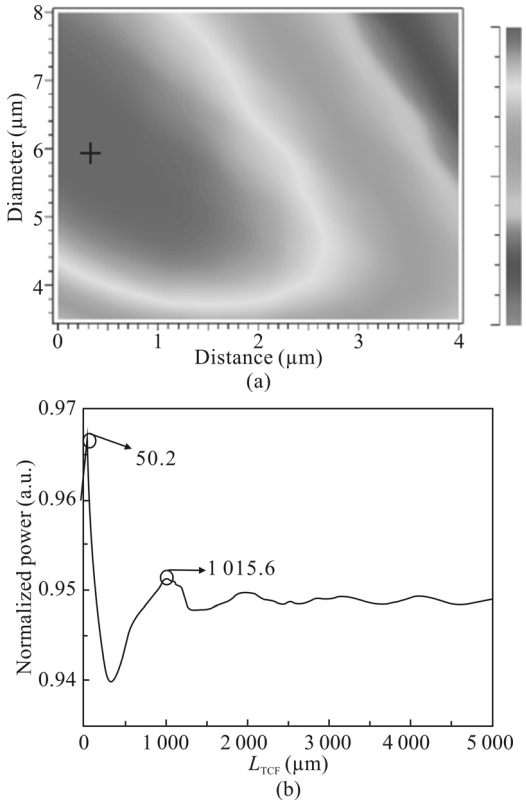

Fig.2 (a) Calculated normalized LP_{11} mode power as a function of both the pitch D and diameter d with L_{TCF}=100 μm; (b) LP_{11} mode power as a function of L_{TCF}, where the pitch D and diameter d are the optimized values indicated by the black cross in (a)

The all-fiber mode convertors based on LPGs often suffer from the drawback of limited bandwidth since the coupling between core/cladding modes is wavelength-dependent. The proposed scheme, however, spatially shapes the incident LP_{01} modes to the LP_{11} mode which is less dependent on the operation wavelength. We use the optimum conditions of the highest conversion efficiency described above and only scan the wavelength, and the results are shown in Fig.3. A wide wavelength range from 1.3 μm to 1.6 μm for different L_{TCF} (including the best value of 50.2 μm) with overall conversion efficiency greater than 93% is demonstrated in Fig.3. And the inset presents the converted LP_{11} mode profile in the FMF at 1.55 μm.

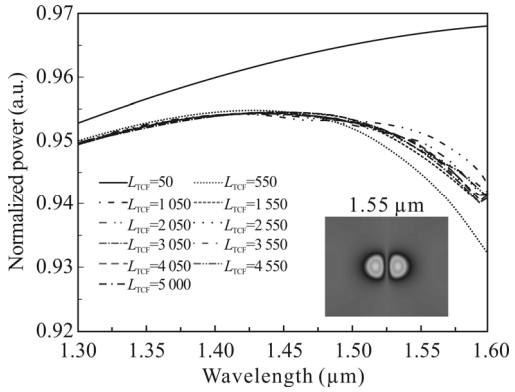

Fig.3 Dependence of the normalized power with optimized TCF parameters on wavelength and the converted LP_{11} mode profile at 1.55 μm

The mode conversion efficiency can be characterized by the coupling loss. Effective mode area can be used to characterize the coupling loss, which is defined as[20]

$$A_{\text{eff}} = \frac{\left(\iint |E|^2 \, \mathrm{d}A\right)^2}{\iint |E|^4 \, \mathrm{d}A}, \tag{2}$$

where E is the electrical field of the specific mode. The coupling loss of the mode convertor is evaluated as

$$\alpha_{\text{Loss}} = 10 \log \left[\frac{4 A_{\text{eff,in}} A_{\text{eff,LP}_{11}}}{\left(A_{\text{eff,in}} + A_{\text{eff,LP}_{11}}\right)^2} \right]. \tag{3}$$

Two FEM models are built which individually refer to the TCF and FMF. The physical parameters of the TCF are the optimum values for the highest conversion efficiency, while those of the FMF are in Tab.1. The calculated effective mode areas of the four degenerate LP_{11} modes in the FMF and the first four possible modes in the TCF are shown in Fig.4(a). The degenerate LP_{11} modes almost have the same effective mode area from 1.3 μm to 1.7 μm. As for the TCF, although we have four solutions, the electrical field distributions indicate that the first and third ones are non-existent in practice. The electrical fields of the remaining two solutions are given by the insets. It's obvious that only the second TCF mode has the similar spatial profile and closer effective mode area to the LP_{11} modes. Eventually, the calculated coupling loss from the second TCF mode to degenerate LP_{11} modes according to Eq.(3) is shown in Fig.4(b). Overall coupling loss less than 0.1 dB from 1.3 μm to 1.7 μm is successfully demonstrated. The insets present the electrical field of the corresponding LP_{11} mode.

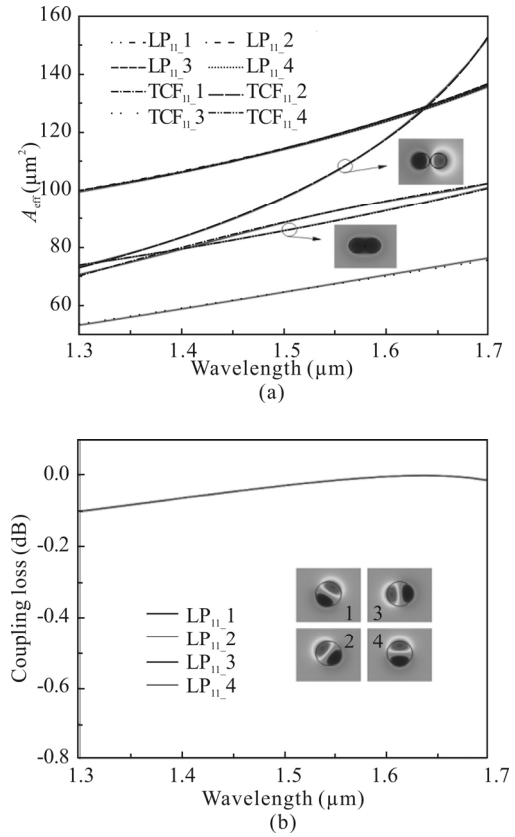

Fig.4 (a) Effective mode areas of the LP_{11} modes in the FMF and the first four modes of the TCF (Inset is the electrical field of the second mode supported by the TCF.); (b) Coupling loss of the second TCF mode to each LP_{11} spatial mode (Inset shows the electrical field of each LP_{11} mode, and black circles represent the core/cladding.)

The conversion efficiency of the proposed all-fiber mode convertor is dependent on the match degree of the input profile from the TCF and the LP_{11} mode profile supported by the FMF. The diameter of the FMF is of great concern with respect to the conversion efficiency and fabrication tolerance. In the BPM model, the parameters of the small core fibers are the optimized ones from previous simulations and the diameter of the FMF is scanned from 13 μm to 39 μm. The results are given in Fig.5. In Fig.5, the normalized power is referred to the power of the LP_{11} mode at the output end of the structure. In this way, the normalized LP_{11} mode power is equal to the conversion efficiency. As we can see from Fig.5, the conversion efficiency is gradually decreased from 93.7% to 38.4%. The insets show the converted mode profiles at

the corresponding diameters indicated by the number on the top right. The supported LP_{11} mode profile varies as the FMF diameter, but the input profile from the TCF maintains the optimized LP_{11} profile of 13 μm FMF diameter. Therefore, mismatched profiles result in low conversion efficiency. However, the points in the box in Fig.5 show the conversion efficiencies are greater than 90% even with 17.8 μm FMF diameter, indicating promising mismatched tolerance.

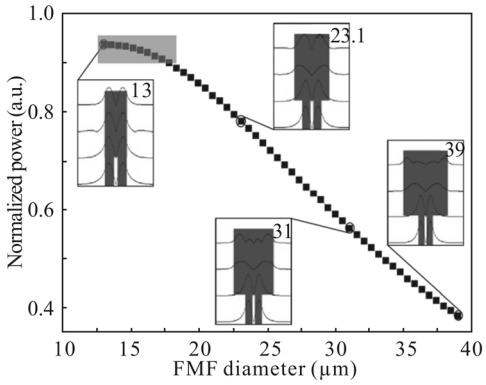

Fig.5 The conversion efficiency as a function of the FMF diameter

We have numerically demonstrated an all-fiber LP_{01}-LP_{11} mode convertor with side-polished small-core SMFs. The side-polished parts merge into an equivalent TCF that spatially shapes the incident LP_{01} modes to the LP_{11} mode. The highest conversion efficiency is 96.7% at 1.55 μm with optimum conditions of 0.32 μm pitch distance, 5.97 μm TCF core diameter and 50.2 μm TCF length, respectively. The proposed convertor works in a wide wavelength range from 1.3 μm to 1.7 μm with overall conversion efficiency greater than 95% and overall coupling loss less than 0.1 dB. Such an all-fiber compact mode convertor may find applications in novel MDM systems.

References

[1] Li A., Chen X., Amin A. A., Ye J. and Shieh W., Journal of Lightwave Technology **30**, 3953 (2012).

[2] Ryf R., Randel S., Gnauck A. H., Bolle C., Sierra A. and Mumtaz S., Journal of Lightwave Technology **30**, 521 (2012).

[3] Nagaraj K. K. C. and Kahn J., Journal of Lightwave Technology **99**, 1 (2017).

[4] Richardson D. J., Fini J. M. and Nelson L. E., Nat. Photon. **7**, 354 (2013).

[5] G. Li, N. Bai, N. Zhao and C. Xia, Advances in Optics and Photonics **6**, 413 (2014).

[6] Nakajima K., Matsui T., Saito K., Sakamoto T. and Araki N., Itu Kaleidoscope: Icts for A Sustainable World, IEEE, 1 (2017).

[7] Randel S., Ryf R., Sierra A., Winzer P. J., Gnauck A. H. and Bolle C. A., Opt. Express **19**, 16697 (2011).

[8] Carpenter J., Thomsen B. C. and Wilkinson T. D., Journal of Lightwave Technology **30**, 3946 (2012).

[9] Carpenter J. and Wilkinson T. D., Journal of Lightwave Technology **30**, 1978 (2012).

[10] Franz B. and Bulow H., IEEE Photonics Technology Letters **24**, 1363 (2012).

[11] Andermahr N. and Fallnich C., Optics Express **18**, 4411 (2010).

[12] Giles I., Obeysekara A., Rongsheng C., Giles D., Poletti F. and Richardson D., IEEE Photonics Technology Letters **24**, 1922 (2012).

[13] Li A., Xi C., Al Amin A. and Shieh W., 2012 IEEE Photonics Society Summer Topical Meeting Series, 197 (2012).

[14] Lai K., Leon-Saval S., Witkowska A., Wadsworth W. and Birks T., Optics Letters **32**, 328 (2007).

[15] Witkowska A., Leon-Saval S. G., Pham A. and Birks T. A., Optics Letters **33**, 306 (2008).

[16] Liu Z., Wang L., Liang P., Zhang Y., Yang J. and Yuan L., Optics Letters **38**, 2617 (2013).

[17] Ryf R., Fontaine N. K. and Essiambre R. J., IEEE Photonics Technology Letters **24**, 1973 (2012).

[18] Tsekrekos C. P. and Syvridis D., IEEE Photonics Technology Letters **24**, 1638 (2012).

[19] Lefevre H. C., Electronics Letters **16**, 778 (1980).

[20] Agrawal G. P., Nonlinear Fiber Optics, Academic Press, 2007.